

Supplementary Information

Evidence of Dynamical Effects in a Cobalt Spin Crossover Complex

Thilini K.Ekanayaka^a, Ping Wang^b, Saeed Yazdani^c, Jared Paul Phillip^c, Esha Mishra^a, Ashley S. Dale^c, Alpha T. N'Diaye^d, Christoph Klewe^d, Pdraic Shafer^d, John Freeland^c, Robert Streubel^a, James Paris Wampler^f, Vivien Zapf^f, Ruihua Cheng^c, Michael Shatruk^b, Peter A. Dowben^a

a. Department of Physics and Astronomy, Jorgensen Hall, University of Nebraska, Lincoln, NE 68588, U.S.A.

b. Department of Chemistry and Biochemistry, Florida State University, 95 Chieftan Way, Tallahassee, FL 32306, U.S.A.

c. Department of Physics, Indiana University-Purdue University Indianapolis, Indianapolis, Indiana 46202, U.S.A.

d. Advanced Light Source, Lawrence Berkeley National Laboratory, Berkeley, CA 94720, U.S.A.

e. Argonne National Laboratory, Advanced Photon Source, Bldg. 431/E003, 9700 South Cass Ave., Argonne IL 60439, U.S.A.

f. Los Alamos National Laboratory, P.O. Box 1663, Los Alamos, NM 87545, U.S.A.

Further Experiment Details:

[Co(SQ)(Cat)(4-CN-py)₂] was synthesized according to previously published procedures.¹⁻⁴ Briefly, a solution of 4-CN-py (95 mg, 0.91 mmol) in 20 mL of toluene was added to a solution of [Co^{II}(SQ)₂]₄ (226 mg, 0.11 mmol) in 70 mL of toluene (70 mL). The resulting solution was stirred at 35°C for 5 h in the dark, after which the solution was filtered and the filtrate was slowly evaporated by purging with a flow of N₂ gas, to crystallize [Co(SQ)(Cat)(4-CN-py)₂] as dark-blue needles. Yield = 69% (based on [Co^{II}(SQ)₂]₄).

The 100 nm-thick [Co(SQ)(Cat)(4-CN-py)₂] thin films were synthesized using the solution of 5 mg of [Co(SQ)(Cat)(4-CN-py)₂] in 16 mL of toluene and drop-casting 50 μL on a highly oriented pyrolytic graphite (HOPG) substrate, applied nearly perpendicular to the sample. The X-ray magnetic circular dichroism (XMCD) spectra were created from individual X-ray absorption spectra were taken at both positive and negative applied magnetic field and subsequently subtracted from each other yielding the final spectrum to eliminate measurement artifacts. While not affecting the XMCD signal, except to decrease the overall signal to noise ratio, the overall XAS and XPS spectra collection in the total electron yield mode is complicated because [Co(SQ)(Cat)(4-CN-py)₂] is quite dielectric with a resistivity around 10⁸ Ω cm. The magnetometry

data was taken in a vibrating sample magnetometer (VSM) with a 14 Tesla Physical Properties Measurement System (PPMS) for temperatures between 2 and 300 K.

Establishing the molecular integrity of $[\text{Co}(\text{SQ})_2(4\text{-CN-py})_2]$

Raman spectroscopy was employed as one method to confirm that the complex stayed intact after thin film deposition. As shown in Figure S1, the thin-film samples exhibit the $\nu(\text{CN})$ value of 2327 cm^{-1} for $[\text{Co}(\text{SQ})(\text{Cat})(4\text{-CN-py})_2]/[\text{Co}(\text{SQ})_2(4\text{-CN-py})_2]$ on the HOPG or Si substrate, which is nearly identical to the $\nu(\text{CN})$ value of 2328 cm^{-1} observed for the bulk $[\text{Co}(\text{SQ})(\text{Cat})(4\text{-CN-py})_2]/[\text{Co}(\text{SQ})_2(4\text{-CN-py})_2]$. These values are drastically different from 2244 cm^{-1} observed for the free 4-CN-py ligand. Thus, the results of Raman spectroscopy indicate that the complex does not dissociate when converted to the thin-film samples by drop-casting.

X-ray diffraction (Figure S2) shows no shift in the diffraction peaks when comparing the $[\text{Co}(\text{SQ})(\text{Cat})(4\text{-CN-py})_2]/[\text{Co}(\text{SQ})_2(4\text{-CN-py})_2]$ powder and after thin film deposition. This finding is also consistent with $[\text{Co}(\text{SQ})(\text{Cat})(4\text{-CN-py})_2]/[\text{Co}(\text{SQ})_2(4\text{-CN-py})_2]$ remaining intact after thin film deposition.

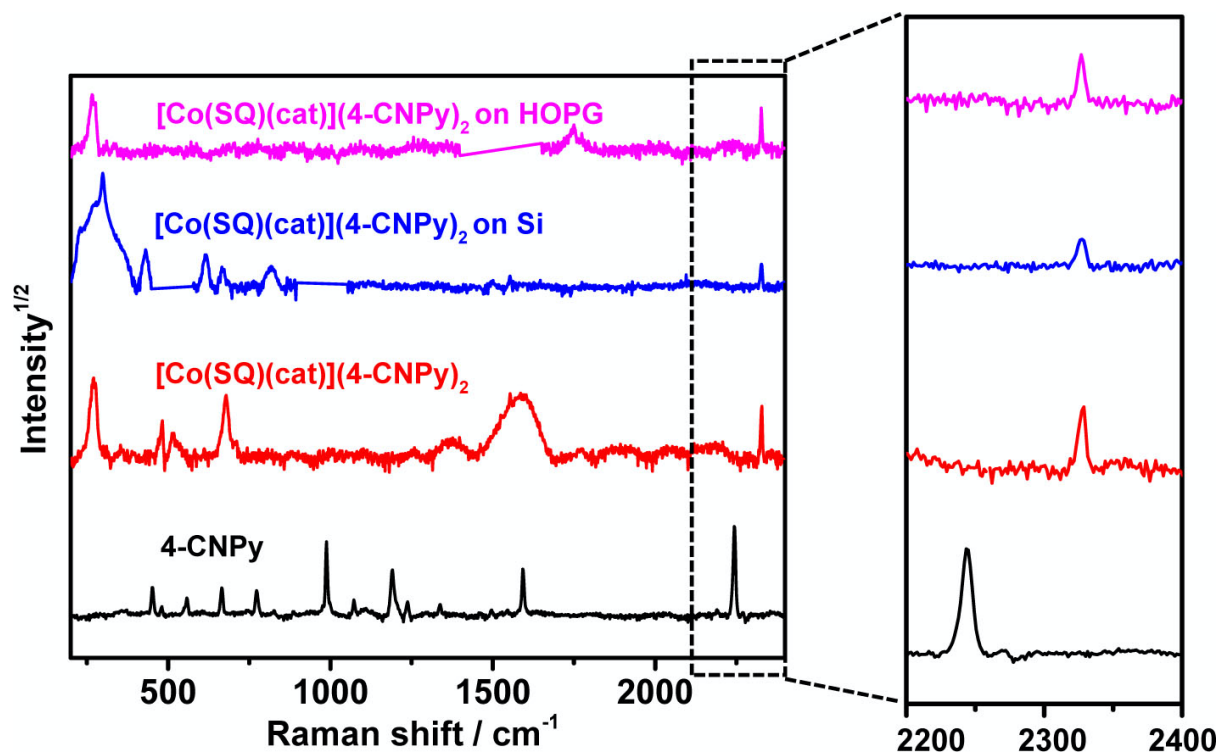


Figure S1: Raman spectra taken for $[\text{Co}(\text{SQ})(\text{Cat})(4\text{-CN-py})_2]/[\text{Co}(\text{SQ})_2(4\text{-CN-py})_2]$ powder, the cyano-pyridine ligand and for thin $[\text{Co}(\text{SQ})(\text{Cat})(4\text{-CN-py})_2]/[\text{Co}(\text{SQ})_2(4\text{-CN-py})_2]$ films deposited on HOPG and SiO_2 and Pyridine ligand.

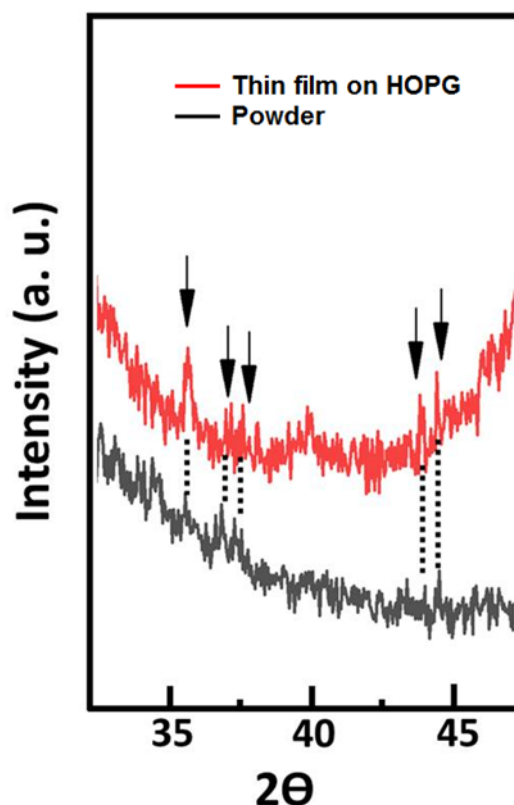


Figure S2: XRD measurements of $[\text{Co}(\text{SQ})(\text{Cat})(4\text{-CN-py})_2]/[\text{Co}(\text{SQ})_2(4\text{-CN-py})_2]$ powder compared with the $[\text{Co}(\text{SQ})(\text{Cat})(4\text{-CN-py})_2]/[\text{Co}(\text{SQ})_2(4\text{-CN-py})_2]$ thin film deposited on HOPG.

Possible variations in the critical field for the orbital moment of $[\text{Co}(\text{SQ})_2(4\text{-CN-py})_2]$

The persistence of $[\text{Co}(\text{SQ})_2(4\text{-CN-py})_2]$ in the HS state, in the presence of X-ray fluence across a wide range of temperatures, permits a comparison of the spin and orbital moments using XMCD spectroscopy. The orbital moment appears to have a nonzero critical field, and while there is a range in the estimate of the critical field varies using a jack-knife indicator, i.e. repeating the fitting of orbital moments while excluding one data point at a time, in no case is the critical field zero.

The existence of a nonzero critical field suggests a preferential orientation of $[\text{Co}(\text{SQ})_2(4\text{-CN-py})_2]$ thin films in the high spin state on graphite at 200 K. There is, however, no low energy electron diffraction (LEED), X-ray diffraction (XRD), or scanning tunnelling microscopy (STM) available at present to confirm any assertion regarding a preferential orientation. As noted in the experimental, is very dielectric with a resistance greater than $10^8 \Omega\cdot\text{cm}$, hindering the acquisition of both LEED and STM. However, in spite nominally octahedral bonding configuration, symmetry is broken within the molecule and by the substrate and through nearest neighbor interactions. So

cobalt is not actually in a perfect octahedral environment. The surface potential and the electric field across the molecule substrate interface ensure that thin molecular film sits within an electric field that will influence the molecular dipole.

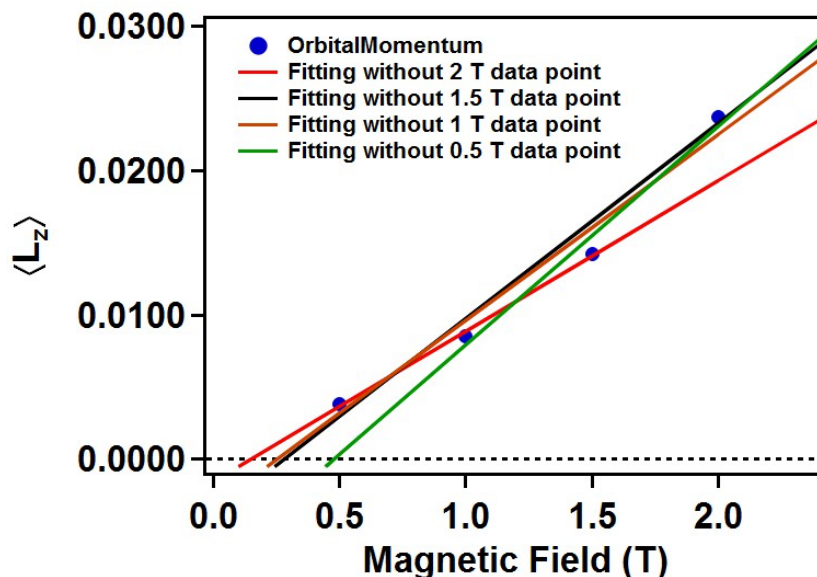


Figure S3: The least squares linear fitting of orbital moments to the data, after excluding one data point at a time. These family of fittings clearly indicates that none of these fittings go through zero. This confirms that there is a critical field barrier for $[\text{Co}^{\text{II}}(\text{SQ})_2(4\text{-CN-py})_2]$ thin films, in the high spin state, on graphite at 200 K.

Resistivity

While not affecting the XMCD signal, the overall XAS and XPS spectra collection in the total electron yield mode is complicated because $[\text{Co}^{\text{II}}(\text{SQ})_2(4\text{-X-py})_2]$ is quite dielectric. In-plane transport measurements were done using a Keithley 6487 Picoammeter for a thin film of $[\text{Co}^{\text{II}}(\text{SQ})_2(4\text{-X-py})_2]$ deposited directly on prepatterned Au electrodes 250 nm thick and 10 μm wide with an intradigitated spacing of 5 μm , as shown in Figure S4. The I-V measurement taken for 128 nm film of $[\text{Co}^{\text{II}}(\text{SQ})_2(4\text{-X-py})_2]$ at room temperature indicate a resistivity greater than $10^8 \Omega \text{ cm}$. This indicates that this molecule is a highly dielectric material, making it difficult to acquire XAS and XPS spectra for this system. In passing, as noted elsewhere,⁵ this very high resistance reduces the efficacy of $[\text{Co}^{\text{II}}(\text{SQ})_2(4\text{-X-py})_2]$ for a spin crossover memory device.

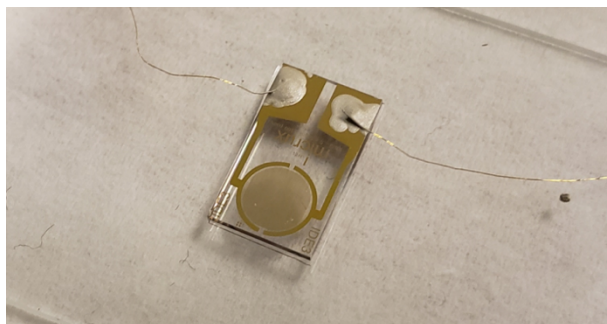


Figure S4: The Au intradigit electrodes system used for the transport measurements

Retention of the high spin state with temperature during XAS

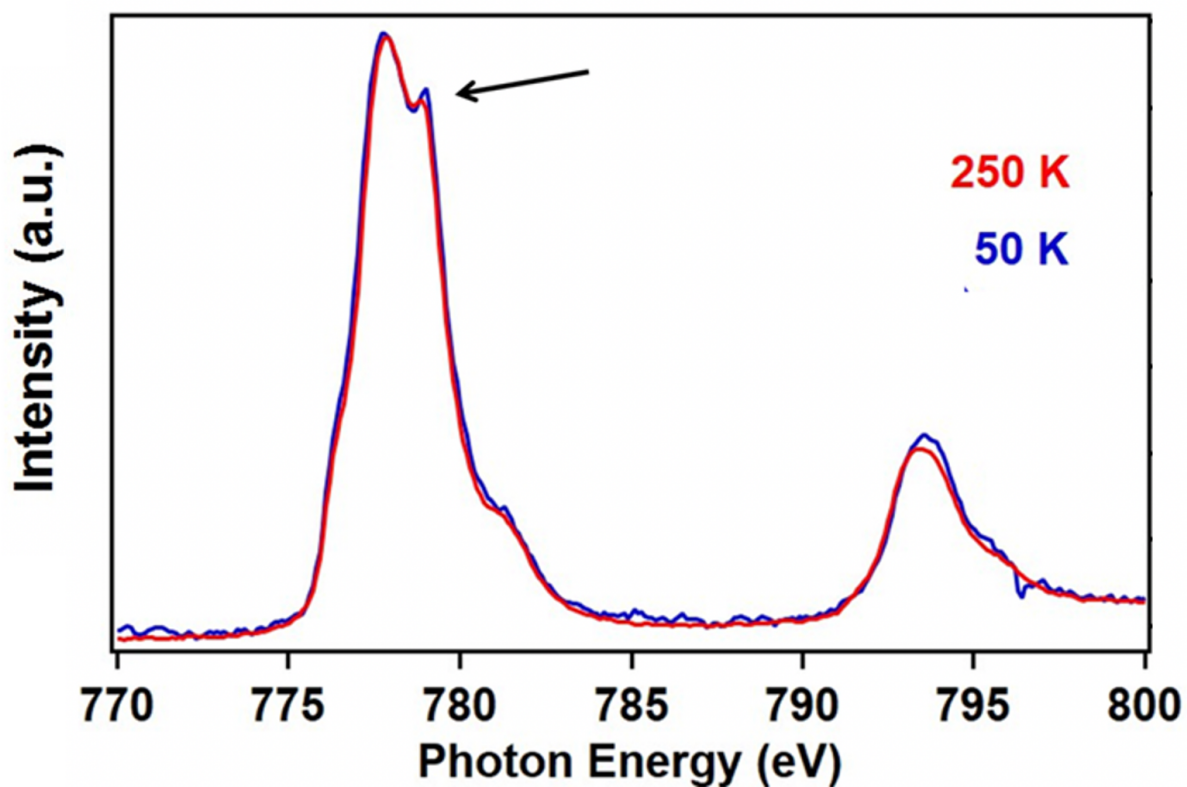


Figure S5: The XAS spectra of $[\text{Co}^{\text{II}}(\text{SQ})_2(4\text{-X-py})_2]$ taken in the TEY mode at 50 K to 250 K. The small changes due to temperature are indicated by the arrow.

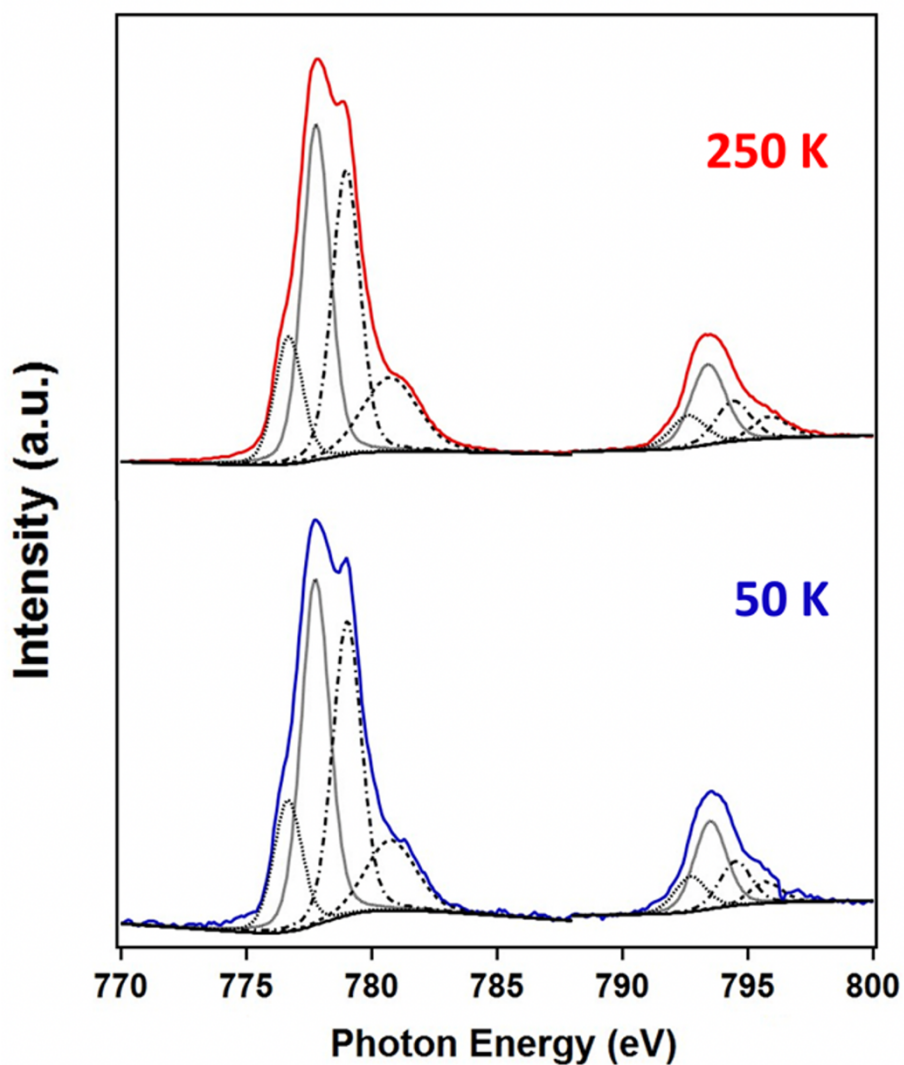


Figure S6: The XAS spectrums at 50 K and 250 K, with the component fittings shown.

References:

- [1] R. D. Schmidt, D. A. Shultz and J. D. Martin, *Inorg. Chem.*, 2010, **49**, 3162–3168.
- [2] R. D. Schmidt, D. A. Shultz, J. D. Martin and P. D. Boyle, *J. Am. Chem. Soc.*, 2010, **132**, 6261–6273.
- [3] T. M. Francisco, W. J. Gee, H. J. Shepherd, M. R. Warren, D. A. Shultz, P. R. Raithby and C. B. Pinheiro, *J. Phys. Chem. Lett.*, 2017, **8**, 4774–4778.

- [4] M. A. Ribeiro, D. E. Stasiw, P. Pattison, P. R. Raithby, D. A. Shultz and C. B. Pinheiro, *Crystal Growth & Design*, 2016, **16**, 2385–2393.
- [5] T. K. Ekanayaka, G. Hao, A. Mosey, A. S. Dale, X. Jiang, A. J. Yost, K. R. Sapkota, G. T. Wang, J. Zhang, A. T. N'Diaye, A. Marshall, R. Cheng, A. Naeemi, X. Xu, and P. A. Dowben, *Magnetochemistry*, 2021, **7**, 37.